The Astrophysical Journal, 1001:178 (11pp), 2026 April 20 https://doi.org/10.3847/1538-4357/ae5488

Exploring MAXI J1744−294: IXPE Insights into a Galactic Center X-Ray Transient

Lorenzo Marra[1], Romana Mikušincová[1], Federico M. Vincentelli[1], Fiamma Capitanio[1], Melania Del Santo[2], Sergio Fabiani[1], Shifra Mandel[3,24], Fabio Muleri[1], Maxime Parra[4], Paolo Soffitta[1], Antonella Tarana[1], M. Cristina Baglio[5], Stefano Bianchi[6], Stéphane Corbel[7], Enrico Costa[1], Antonino D'Aì[2], Barbara De Marco[8], Michal Dovčiak[9], Vittoria Elvezia Gianolli[10], Andrea Gnarini[6,11], Maitrayee Gupta[9], Adam Ingram[12], Guglielmo Mastroserio[13], Giorgio Matt[6], Kaya Mori[3], Pierre-Olivier Petrucci[14], Jakub Podgorný[9], Juri Poutanen[15], James F. Steiner[16], Jiří Svoboda[9], Roberto Taverna[17], Francesco Tombesi[18], Swati Ravi[19], Jérôme Rodriguez[20,21], Thomas D. Russell[2], Alexandra Veledina[15,22], and Shuo Zhang[23]

[1] INAF, Istituto di Astrofisica e Planetologia Spaziali, Via del Fosso del Cavaliere 100, 00133 Roma, Italy; lorenzo.marra@inaf.it
[2] INAF, Istituto di Astrofisica Spaziale e Fisica Cosmica, Via U. La Malfa 153, I-90146 Palermo, Italy
[3] Columbia Astrophysics Laboratory, Columbia University, New York, NY 10027, USA
[4] Department of Physics, Ehime University, 2-5, Bunkyocho, Matsuyama, Ehime 790-8577, Japan
[5] INAF, Osservatorio Astronomico di Brera, Via Bianchi 46, I-23807 Merate (LC), Italy
[6] Dipartimento di Matematica e Fisica, Università degli Studi Roma Tre, Via della Vasca Navale 84, 00146, Roma, Italy
[7] Université Paris Cité, Université Paris-Saclay, CEA, CNRS, AIM, F-91191 Gif-sur-Yvette, France
[8] Departament de Fisíca, EEBE, Universitat Politècnica de Catalunya, Av. Eduard Maristany 16, S-08019 Barcelona, Spain
[9] Astronomical Institute of the Czech Academy of Sciences, Boční II 1401/1, 14100, Praha 4, Czechia
[10] Department of Physics and Astronomy, Clemson University, Clemson, SC 29634, USA
[11] NASA Marshall Space Flight Center, Huntsville, AL 35812, USA
[12] School of Mathematics, Statistics, and Physics, Newcastle University, Newcastle upon Tyne NE1 7RU, UK
[13] Dipartimento di Fisica, Univerusità Degli Studi di Milano, Via Celoria, 16, Milano, 20133, Italy
[14] University Grenoble Alpes, CNRS, IPAG, 38000 Grenoble, France
[15] Department of Physics and Astronomy, 20014, University of Turku, Finland
[16] Center for Astrophysics | Harvard-Smithsonian, 60 Garden Street, Cambridge, MA 02138, USA
[17] Dipartimento di Fisica e Astronomia, Università degli Studi di Padova, Via Marzolo 8, 35131 Padova, Italy
[18] Department of Physics, Tor Vergata University of Rome, 00133 Rome, Italy
[19] MIT Kavli Institute for Astrophysics and Space Research, 77 Massachusetts Avenue, Cambridge, MA 02139, USA
[20] Université Paris-Saclay, Université Paris Cité, CEA, CNRS, AIM, F9119, Gif Sur Yvette, France
[21] Observatoire des Sciences de l'Univers de l'université Paris-Saclay, Bât. 121, 91405 Orsay, France
[22] Nordita, KTH Royal Institute of Technology and Stockholm University, Hannes Alfvéns väg 12, SE-10691 Stockholm, Sweden
[23] Michigan State University, Department of Physics and Astronomy, East Lansing, MI 48824, USA
Received 2025 June 20; revised 2026 March 16; accepted 2026 March 16; published 2026 April 15

Abstract

We present the first IXPE spectro-polarimetric observation of the black hole candidate MAXI J1744−294, a transient X-ray source observed during a bright 2025 outburst in the Galactic center region. The source has recently been identified as most likely a repeat outburst of the 2016 transient Swift J174540.2−290037. During the ∼150 ks observation, the source was detected in the soft state, and its spectrum was well described by an absorbed multicolor disk with a minor high-energy tail. We did not detect any significant polarization from the source, and hence we derived a 3σ upper limit on the polarization degree of 1.3% in the 2–8 keV energy band. This result is consistent with previous findings for soft-state black hole binaries observed at low to intermediate inclination angles. By comparing the polarization degree upper limit with theoretical predictions for standard accretion disk emission, we constrain the disk inclination to $i \lesssim 38°$–$72°$, depending on the black hole spin and the disk atmosphere albedo, consistent with inclination estimates obtained during the 2016 outburst of Swift J174540.2−290037.

Unified Astronomy Thesaurus concepts: Polarimetry (1278); X-ray astronomy (1810); X-ray binary stars (1811); Stellar mass black holes (1611)

Materials only available in the online version of record: data behind figures

1. Introduction

Stellar mass black holes (BHs) in X-ray binary (XRB) systems serve as natural laboratories for investigating accretion physics, relativistic jet formation, and the effects of strong gravitational fields. These systems host a BH (5–30 $M_\odot$) accreting matter from a companion star via an accretion disk (K. Belczynski et al. 2010; J. M. Corral-Santana et al. 2016). While a subset of these sources remains persistently active over extended periods of time, the majority exhibit transient behavior, cycling between long phases of quiescence and dramatic outbursts (A. R. King et al. 1996; J. M. Corral-Santana et al. 2016; B. E. Tetarenko et al. 2016). During these outbursts, the X-ray luminosity increases by several orders of magnitude (W. Yu & Z. Yan 2009), providing a unique opportunity to study accretion processes across a wide range of physical scales.

[24] National Science Foundation Fellow.

A defining characteristic of BH XRBs is the pronounced variability in their spectral and timing properties throughout an outburst (e.g., T. M. Belloni 2010). During these events sources trace a characteristic q-shaped path in the hardness-intensity diagram (HID; R. P. Fender et al. 2004; J. Homan & T. Belloni 2005), transiting through a sequence of spectral states that are interpreted as manifestations of changes in the accretion flow geometry and radiative mechanisms (A. A. Zdziarski & M. Gierliński 2004; C. Done et al. 2007). The outburst generally begins in the hard state, where the spectrum is characterized by a cutoff power law with an energy roll-over at ∼100 keV, typically attributed to Comptonization of soft disk photons by a hot, optically thin medium (the corona; K. S. Thorne & R. H. Price 1975; R. A. Sunyaev & J. Truemper 1979; C. Done et al. 2007). As the luminosity increases, the system evolves through intermediate states into the soft state, in which the emission is dominated by a multicolor blackbody component, generally interpreted as thermal emission from a geometrically thin, optically thick accretion disk extending down to the innermost stable circular orbit (ISCO; I. D. Novikov & K. S. Thorne 1973; N. I. Shakura & R. A. Sunyaev 1973; D. N. Page & K. S. Thorne 1974; K. Mitsuda et al. 1984; K. Makishima et al. 1986).

These transitions, which typically occur on timescales of hours to days, are thought to be primarily driven by variations in the mass accretion rate, even though a second parameter (still unknown) must be at play to explain the hysteretic behavior of the outburst (T. M. Belloni 2010; R. J. H. Dunn et al. 2010; B. E. Tetarenko et al. 2016). In particular, the hard-to-soft transition takes place at higher luminosities than the reverse soft-to-hard transition, producing the characteristic hysteresis loop in the HID (T. J. Maccarone & P. S. Coppi 2003; E. Meyer-Hofmeister et al. 2005). Despite extensive observational and theoretical work, the physical origin of this hysteresis remains a critical puzzle. Intermediate states and fast transitions (T. Belloni et al. 2005; M. Del Santo et al. 2009), failed-transition outbursts (F. Capitanio et al. 2009; T. Bassi et al. 2019; K. Alabarta et al. 2021), and the state-dependent appearance of outflows such as disk winds (G. Ponti et al. 2012; M. Parra et al. 2024) and radio jets (R. P. Fender et al. 2004) further complicate the picture.

A promising avenue to disentangle these complexities is via X-ray polarimetry, which provides direct insights into the geometry and emission mechanisms of the accretion flow. This approach has become possible with the launch of the Imaging X-ray Polarimetry Explorer (IXPE) in 2021 (M. C. Weisskopf et al. 2022), enabling the first systematic measurements of X-ray polarization from BH XRBs in the 2–8 keV energy band. Polarization measurements of sources in the soft state can provide an additional way to constrain the spin of a BH (P. A. Connors & R. F. Stark 1977; R. F. Stark & P. A. Connors 1977; P. A. Connors et al. 1980; M. Dovčiak et al. 2008; J. D. Schnittman & J. H. Krolik 2009; R. Taverna et al. 2020), while observations in the hard state offer unprecedented insights into the geometry of the corona, e.g., in comparison to the jet and the accretion-disk orientation (J. Poutanen & R. Svensson 1996; J. D. Schnittman & J. H. Krolik 2010; H. Krawczynski & B. Beheshtipour 2022; W. Zhang et al. 2022).

IXPE has observed both persistent and transient BH XRBs across various spectral states (see M. Dovčiak et al. 2024, for a recent review). Observations of the persistent XRB Cyg X-1 in the hard state (H. Krawczynski et al. 2022; V. Kravtsov et al. 2025) revealed that the polarization direction is aligned with the radio jet, suggesting that the corona is extended perpendicularly to the disk symmetry axis. Similar behavior was observed during the hard-to-soft transitions of GX 339−4 (G. Mastroserio et al. 2025) and Swift J1727.8−1613 (A. Veledina et al. 2023; A. Ingram et al. 2024). The very large polarization degree (PD) recently detected in the hard state observation of the transient source IGR J17091−3624 (9.1% ± 1.6%; M. Ewing et al. 2025) suggests a high inclination angle for this system. However, the unknown orientation of its radio jet currently prevents a direct comparison with the polarization vector direction. Subsequent IXPE observations of Swift J1727.8−1613 during its outburst revealed a gradual decrease in the PD as the source transitioned toward the soft state, a very low PD in the soft state (J. Svoboda et al. 2024a), and a reacquisition of PD during the reverse transition back to the hard state (J. Podgorný et al. 2024). These findings suggest that the corona may retain a similar geometric structure in both the bright and the dim hard states.

For some sources observed in soft state, only an upper limit on the PD could be established (e.g., LMC X-1, J. Podgorný et al. 2023, and GX 339−4, G. Mastroserio et al. 2025). Polarization measurements of LMC X-3 (J. Svoboda et al. 2024b), 4U 1957+11 (L. Marra et al. 2024), and Cyg X-1 (J. F. Steiner et al. 2024) enabled the first BH spin estimates through polarimetric analysis, which yielded results consistent with those obtained by other spectroscopic methods.

A very large PD with a direction perpendicular to the radio jet was observed in Cyg X-3, varying from ∼10% to ∼20% across different spectral states (A. Veledina et al. 2024a, 2024b), suggesting that the source is surrounded by optically thick material—likely a dense wind from the accretion disk—and allowing constraints to be placed on the geometry of the obscuring material. Finally, an unanticipated result came from the soft-state observation of the transient source 4U 1630−47 (A. Ratheesh et al. 2024), followed by its observation in the steep power-law state (N. Rodriguez Cavero et al. 2023). While radio jet emission has recently been detected from this source (I. Mariani et al. 2025), it remains unresolved, so the orientation of the system is still unknown. The very high polarization level measured in the soft state (≈8%), increasing with energy, is difficult to reconcile with the standard accretion-disk model and underscores the need for further theoretical work to understand the physical processes in this source.

1.1. Discovery of the 2025 Outburst

On 2025 January 2 (MJD 60677), the MAXI/GSC all-sky monitor (M. Matsuoka et al. 2009) reported a bright hard X-ray transient near the Galactic center region, initially detected at 10–20 keV with an average flux of ∼100 mCrab and later rising to ∼250 mCrab during 2025 January 13–15. The source was provisionally named MAXI J1744−294. Initial analyses placed the transient position within an error ellipse overlapping Sgr A*, leading to a tentative association with the known neutron star XRB KS 1741−293. However, this association was subsequently ruled out due to the source's unusually high flux and a hard spectral shape (Y. Kudo et al. 2025; M. Nakajima et al. 2025).

Table 1
List of Observations

Observatory	Instrument	Observation ID	Start Date	End Date	Net Exposure (ks)
IXPE	Gas Pixel Detector (GPD)	04250301	2025-04-05 07:36:34	2025-04-08 02:09:33	150
Swift	X-Ray Telescope (XRT)	00033979025	2025-04-05 02:53:16	2025-04-05 03:03:56	0.64
NICER	X-Ray Timing Instrument (XTI)	8205140121	2025-04-03 13:38:17	2025-04-03 13:44:03	0.3

To localize and characterize this source, a coordinated X-ray follow-up campaign was initiated. The NinjaSat CubeSat observed the region on 2025 January 16–23, finding a 2–10 keV flux of 22 mCrab with a steep power-law spectrum (photon index $\Gamma \approx 3.1$) and high absorption ($N_{\rm H} \approx (7^{+5}_{-2}) \times 10^{23}\,{\rm cm}^{-2}$; S. Watanabe et al. 2025). The Swift/XRT pointing on February 1 revealed two sources near Sgr A*: a fainter one consistent within 10″ of the known neutron star XRB AX J1745.6−2901 (with a count rate of $\sim$0.2 count s^{-1}) and a brighter, piled-up source (count rate of $\sim$6 count s^{-1}) centered 25″ southeast of Sgr A*. Spectral analysis of the latter suggested it had transitioned to the soft state (characterized by the disk blackbody temperature of $kT \approx 0.8$ keV; C. O. Heinke et al. 2025).

NuSTAR's 22.7 ks Target of Opportunity (ToO) observation on 2025 February 6 confirmed the counterpart at a position within $\sim$20″ of Sgr A*. The spectrum was well described by an absorbed disk blackbody plus power-law model, along with a Gaussian component to fit a broad emission line centered at 6.63 keV ($\sigma \approx 0.2$ keV), evident in the 6–7 keV range (S. Mandel et al. 2025d). Further soft X-ray spectroscopy and timing studies were carried out with NICER on 2025 February 11–12, with a total exposure time of 2.7 ks. Although the observation may include some contribution from AX J1745.6−2901, due to NICER's lack of imaging capability, the measured spectral parameters are consistent (within uncertainties) with those obtained by NuSTAR (G. K. Jaisawal et al. 2025). Simultaneously, a 15-minute-long radio observation with MeerKAT on 2025 January 25 detected a new point source 18″ from Sgr A* and 23″ from the Swift position, confirming the first radio counterpart of MAXI J1744−294 with a peak brightness of $\sim$0.3 Jy (N. Grollimund et al. 2025).

In 2025 March, high-resolution spectroscopy with the XRISM/Resolve instrument (70 ks exposure; S. Mandel et al. 2025e) and X-ray observations with the Wide-field X-ray Telescope (WXT) and Follow-up X-ray Telescope (FXT) on board on the Einstein Probe ($\approx$2.2 ks exposure; Y. Wang et al. 2025) further constrained the spectral shape of this transient, estimating an absorbed flux of $\sim 8.5 \times 10^{-10}\,{\rm erg\,s^{-1}\,cm^{-2}}$ in the 2–10 keV band. A Chandra/ACIS-S ToO on March 9, with an exposure time of 9.3 ks, achieved subarcsecond localization at (R.A., decl.) = (17:45:40.476, −29:00:46.10) ± 1.″2, confirming the source offset by <20″ from Sgr A* (S. Mandel et al. 2025b).

The identification of MAXI J1744−294 as either a new transient or a recurrent outburst has been complicated by its location in the crowded Galactic center environment. While the source was initially identified as a new transient, subsequent comparison with archival Chandra data indicates that MAXI J1744−294 is likely a repeat outburst of the transient Swift J174540.2−290037 (S. Mandel et al. 2025c, 2026), originally discovered during a 2016 outburst (K. Mori et al. 2019). Throughout this work, we refer to the source as MAXI J1744−294, following the naming convention adopted for the 2025 outburst.

The emerging picture for the 2025 outburst of MAXI J1744−294 is that of a bright, heavily absorbed X-ray transient in the crowded environment of the Galactic center. The absence of neutron-star signatures, such as type I thermonuclear bursts, coherent pulsations, or an additional soft thermal component from a stellar surface, is consistent with the source being a BH low-mass XRB undergoing a soft-state outburst, in agreement with the interpretation proposed for the 2016 outburst of Swift J174540.2−290037 (K. Mori et al. 2019). The Galactic center region is known to host a large population of X-ray transients, as revealed through deep Chandra and Swift/XRT monitoring over the past 2 decades (M. P. Muno et al. 2005; N. Degenaar et al. 2015; C. J. Hailey et al. 2018). Within approximately 100 pc of Sgr A*, an estimated 10–15% of all Galactic low-mass XRBs are found, either in quiescence or in outburst, alongside a number of candidate high-mass XRBs (K. Mori et al. 2021; F. Fortin et al. 2024; S. Mandel et al. 2025a). The 2025 outburst of this system further contributes to the growing sample of Galactic center X-ray binaries, providing a new observational window onto both the compact-object density cusp around Sgr A* and the physical mechanisms that trigger XRB outbursts.

In this work, we report on the IXPE ToO observation of MAXI J1744−294, performed in 2025 April while the source was in the soft state, along with simultaneous coverage by the Swift/XRT and NICER instruments. All studied observations are summarized in Table 1, and details on the data reduction and processing are provided in Section 2. The polarization analysis is presented in Section 3, including an assessment of possible contamination from the Galactic center diffuse emission. In Section 4 we report the joint spectral and spectro-polarimetric modeling, while in Section 5 we discuss the implications of our results for the geometry and physical properties of the system. Finally, our main findings are summarized in Section 6.

2. Observation and Data Reduction

The IXPE is the first space mission dedicated to investigating linear polarization in the 2–8 keV energy band (M. C. Weisskopf et al. 2022). It carries three coaligned X-ray telescopes, each integrating a mirror module assembly (B. D. Ramsey et al. 2022) with a gas pixel detector sensitive to polarization (L. Baldini et al. 2021; P. Soffitta et al. 2021). This design enables high-sensitivity measurements of both pointlike and extended sources. The observatory achieves an angular resolution of approximately 30″ (half-power diameter, averaged over the three detector units, DUs; B. D. Ramsey et al. 2022; R. Ferrazzoli et al. 2025); the overlap of the fields of view of the three DUs is circular, with a diameter of 9′. The energy resolution is better than 20% at 6 keV.

IXPE performed a ToO observation of MAXI J1744−294 from 2025 April 5 at 07:36:34 UTC to April 8 at 02:09:33 UTC (OBSID: 04250301), for a total livetime of approximately 150 ks. We downloaded the publicly available Level 1 and Level 2 data from the IXPE archive[25] and analyzed them using both the IXPEOBSSIM software (version 31.0.3; L. Baldini et al. 2022) and the HEASOFT package XSPEC (version 12.15; K. A. Arnaud 1996). The source region was defined using the SAOIMAGEDS 9[26] software. Events were extracted from a circular region with a radius of 60″, centered on the centroid of the source counts for each IXPE detector (R.A. 17:45:42.629, decl. −29:00:36.86). Due to the modest count rate of the source during the observation (≈1.14 count s^{-1} $arcmin^{-2}$ in the selected region), we applied the background rejection procedure described by A. Di Marco et al. (2023). Given the source position near the Galactic center and its proximity to AX J1745.6−2901, we explored several possible background extraction regions, as detailed in Section 3.1. Notably, AX J1745.6−2901, located at ∼1.′3 from MAXI J1744−294, was serendipitously included in the IXPE field of view. The analysis of its polarization properties is presented in R. Mikušincová et al. (2025). The weighted Stokes I, Q, and U spectra were extracted using the `xselect` tool from the HEASOFT package (version 6.35.1) with the command `extract spect stokes=NEFF`. Response files were generated using the `ixpecalcarf` tool on the event and attitude files of each DU, applying the latest available IXPE calibration (v13).[27]

The Swift/X-Ray Telescope (XRT; D. N. Burrows et al. 2005) observed MAXI J1744−294 in Window Timing (WT) mode on 2025 April 5 from 02:53:16 UTC to 03:03:56 UTC (ObsID 00033979025). We reprocessed the XRT data using the task `xrtpipeline` included in the HEASOFT v.6.34 software package and the latest XRT Calibration Database (CALDB v. 20240522). We selected a circular region with a radius of 8 pixels (1 pixel = 2.″36), corresponding to approximately 50% of the point-spread function (PSF), centered on the source position (R.A. 17:45:40.48, decl. −29:00:46.10) to extract the spectra (and response files) using the task `xrtproducts`. We adopted this unconventional radius (8 pixels instead of the standard 20) to reduce contamination from AX J1745.6−2901. Since WT mode data are not affected by pile-up at count rates below approximately 100 count s^{-1}, we extracted the light curve and confirmed that the observation is not impacted by pile-up, with a measured mean count rate of 31 count s^{-1}.

To characterize the temporal behavior of the source, quasi-simultaneous observations in the 0.5–10 keV band were also obtained with NICER on board the International Space Station. The closest observation during nighttime was performed on 2025 April 3 (OBSID: 8205140121) for a total of 300 s. Clean events were extracted using the NICERL2 software (v. 1.36) distributed by HEASARC, with the default parameters. By checking the 10–12 keV light curve, we noticed that the first ≈50 s were affected by high background and thus were excluded from the analysis. Timing analysis was then performed using a rebinned light curve with a time resolution of 1 ms. Due to NICER's lack of imaging capability, however, its data were excluded from the spectral analysis described in Section 4, as it was not possible to reliably disentangle the contribution from AX J1745.6−2901.

[25] https://heasarc.gsfc.nasa.gov/docs/ixpe/archive/
[26] https://sites.google.com/cfa.harvard.edu/saoimageds9
[27] https://heasarc.gsfc.nasa.gov/docs/ixpe/caldb/

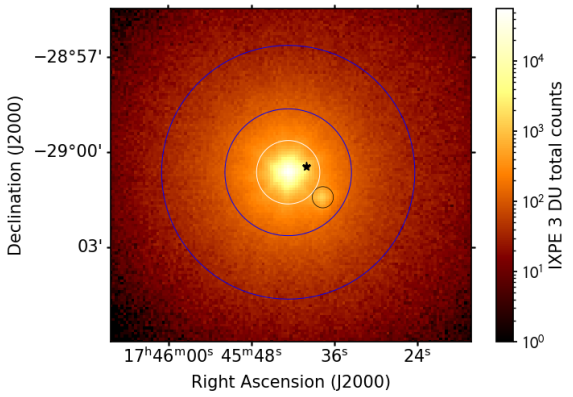

Figure 1. Summed count map of the three IXPE DUs. The color scale is logarithmic to enhance the visibility of both sources and the much fainter background. The white circle indicates the source region used for extraction, while the small black circle located to the lower right of the source region marks the position of AX J1745.6−2901. The blue annulus shows one of the background regions described in Section 3; the alternative configuration uses an annulus extending from the edge of the source region to the same outer radius. The black star indicates the position of Sgr A*.

3. Polarization Measurement

The source and background region used in the extraction of the IXPE data is presented in Figure 1, superimposed to the summed count map of the three IXPE DUs. We initially used the `xpselect` tool from the IXPEOBSSIM software to filter the counts of the MAXI J1744−294 region, and then generated the unweighted polarization cubes in the 2–8 keV band employing the `PCUBE` algorithm of the `xpbin` tool. This analysis revealed a PD lying below the minimum detectable polarization value at the 99% confidence level (MDP_{99}; M. C. Weisskopf et al. 2010), estimated at 1.2% for the observation. At 3σ confidence level only an upper limit on the PD $< 1.9\%$ can be established; consequently, the polarization angle (PA) remains unconstrained. We note that a more stringent 3σ upper limit on the PD can be obtained through weighted spectro-polarimetric fitting, as discussed in Section 4.3.

3.1. Estimate of Background Contamination

We subsequently investigated whether the polarization signal from MAXI J1744−294 could be contaminated by diffuse emission from the Galactic center or by emission from the nearby neutron star transient AX J1745.6−2901. IXPE has previously observed a subset of the molecular clouds composing the Sgr A* complex (F. Marin et al. 2023), revealing a polarization signal in the 4–8 keV range. This signal was attributed to radiation emitted in a past flare of Sgr A* and reflected off the dense clouds in the region, which allowed for an estimation of the flare age at 205^{+50}_{-30} yr. Diffuse emission in the 2–4 keV energy band is instead primarily expected to be unpolarized thermal emission.

To assess whether the diffuse contribution from the Sgr A* complex could affect our observation, we extracted background counts from an annular region centered on the source position. Two configurations were tested: one excluding

AX J1745.6−2901 by selecting inner and outer radii of 120″ and 240″, respectively, and one including it, with inner and outer radii of 60″ and 240″. The PCUBE analysis of both background regions indicates that neither exhibits significant polarization. We derived 3σ PD upper limits of 5.1% for the first configuration and 4.8% for the second (which includes AX J1745.6−2901). In both cases, the background-subtracted PCUBE analysis yielded results consistent with those obtained from the source region, with the PD remaining below MDP_{99}. The estimated upper limits on the PD at the 3σ confidence level are 1.9% and 2.0% for the two configurations, respectively. To further investigate potential contamination from the Galactic center diffuse X-ray emission, we repeated the analysis using a smaller source region with a 30″ radius. The 3σ PD upper limits remained consistent at 2.0%, whether considering only the source region or subtracting either of the two background contributions. Given this consistency across source and background selections, we ultimately adopted the larger source region with a 60″ radius and the background region excluding AXJ1745.6−2901 for the subsequent timing and spectral analyses. These regions are represented by the white circle and blue annulus in Figure 1. We note that a more detailed analysis of the contamination from the Galactic center diffuse emission during the IXPE pointing is discussed in R. Mikušincová et al. (2025).

Energy-resolved polarization analyses similarly showed no significant signal above MDP_{99} in any tested interval. In particular, we estimated a PD upper limit of 2.0% in the 2–4 keV range. In the 4–8 keV band, where F. Marin et al. (2023) reported a detection, we derived a higher 3.4% upper limit, suggesting that any polarization contamination from the Sgr A* complex is negligible. Notably, a lower PD upper limit of 1.6% is found in the 2–6 keV energy band, while a large 14.7% upper limit is estimated between 6 and 8 keV.

Although no significant time-averaged polarization is observed, a time-dependent signal could still be present in the IXPE observation. To investigate this, we computed the normalized Stokes parameters Q/I and U/I in 20 time bins of approximately 7.5 ks, as shown in the two bottom panels of Figure 2. These quantities are expected to behave as independent normal variables (F. Kislat et al. 2015). We fit their temporal evolution with constant models; the resulting null hypothesis probabilities are ∼81% for both Q/I and U/I, indicating that the observed fluctuations are statistically consistent with random noise. We therefore conclude that no significant time variability in polarization is detected.

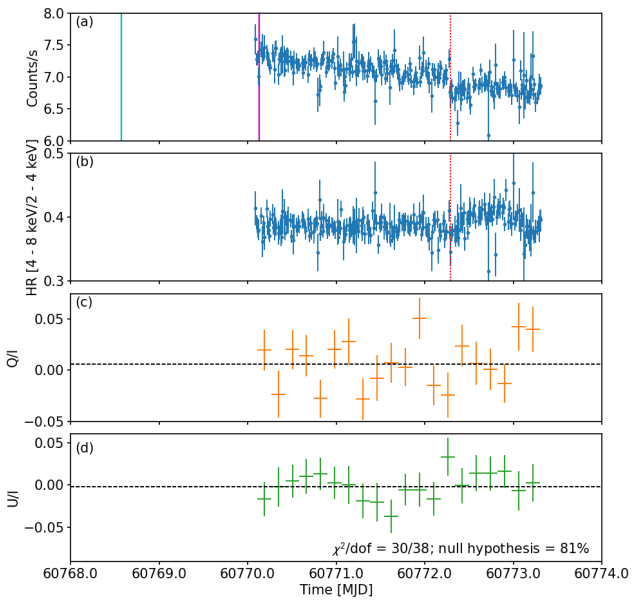

Figure 2. Light curves and time-dependent polarization properties of MAXI J1744−294 from the IXPE observation. (a) IXPE light curve in the 2–8 keV energy range with 800 s time bins. The cyan and magenta vertical regions indicate the time intervals covered by the NICER and Swift/XRT observations, respectively. (b) Time evolution of the hardness ratio, defined as the ratio of IXPE count rates in the 4–8 keV and 2–4 keV bands, using the same 800 s time bins. The vertical dotted red line in panels (a) and (b) highlights the count-rate drop described in Section 4.1. (c, d) Normalized Stokes Q and U parameters, measured by IXPE as a function of time. Dashed lines show the best-fit constant model; the corresponding χ^2, numbers of degrees of freedom, and null hypothesis probabilities are reported in panel (d). (The data used to create this figure are available in the online article.)

4. Spectro-polarimetric Analysis

4.1. Temporal Behavior

During its outburst, MAXI J1744−294 was reported to be in the soft spectral state by several observatories beginning in early 2025 February (C. O. Heinke et al. 2025; S. Mandel et al. 2025d; Y. Wang et al. 2025). By the time of the IXPE observation in early 2025 April, the source flux was gradually declining. The 2–8 keV count rate, shown in the top panel of Figure 2 with 800 s time bins, decreased by approximately 10% over the duration of the observation. The hardness ratio, defined as the ratio of the 4–8 keV count rate to the 2–4 keV count rate and shown in Figure 2(b), remained stable, suggesting that no state transition occurred during the IXPE pointing. A sharp ∼5% drop in the count rate was detected on 2025 April 7 at approximately 06:57 UTC (MJD 60772.29), highlighted in Figure 2(a) by a vertical red dotted line. Coinciding with this event, a slight hardening in the spectrum is hinted at by the hardness ratio; however, given IXPE's narrow energy band, no firm conclusions can be drawn. To assess any possible polarization associated with this variability, we divided the observation into two segments, before and after the drop, but in both intervals no polarization signal was detected. We refer to S. Mandel et al. (2025c) for a more detailed investigation of this event with the analysis of a simultaneous NuSTAR dataset.

To analyze the possible variability of the source, we used the NICER light curve with 1 ms time resolution in the 0.5–10 keV band. While the short exposure allows us to study variability on timescales of only a few minutes, the light curve did not show any sign of stochastic variability. This was also clear from the Fourier analysis. The power density spectrum, computed using the numerical recipe described in P. Uttley et al. (2014) with 8192 bin per segments (i.e., minimum frequency ≈ 0.122 Hz), showed a flat behavior, consistent with only white noise. After subtracting the Poisson noise contribution, we estimate an rms between 0.122 and 500 Hz of ≈3%. While we cannot exclude that the NICER data are contaminated by emission from the nearby source AX J1745.6−2901, the absence of stochastic variability and the low fractional rms indicate that no source within the NICER field of view exhibits temporal features characteristic of the hard state.

Table 2
Best-fit Parameters (with 90% Confidence Uncertainties) of the Joint IXPE and Swift/XRT Spectral Modeling Using the Combined Models Described in Section 4

Component	Parameter (unit)	Description	Value Fit 1	Value Fit 2
tbabs	$N_{\rm H}$ (10^{22} cm^{-2})	Hydrogen column density	$19.2^{+0.6}_{-0.3}$	$19.3^{+0.4}_{-0.3}$
diskbb	$kT_{\rm bb}$ (keV)	Inner disk temperature	0.64 ± 0.01	⋯
	norm (10^4)	Normalization	$1.01^{+0.12}_{-0.10}$	⋯
	$F_{2-8{\rm keV}}$ (10^{-10}ergs^{-1}cm^{-2})	Absorbed flux 2–8 keV	12.46 ± 0.07	⋯
	Flux fraction$_{2-8{\rm keV}}$ (%)	Disk contribution	76	⋯
	$F_{2-6{\rm keV}}$ (10^{-10}ergs^{-1}cm^{-2})	Absorbed flux 2–6 keV	11.89 ± 0.07	⋯
	Flux fraction$_{2-6{\rm keV}}$ (%)	Disk contribution	81	⋯
	$F_{6-8{\rm keV}}$ (10^{-10}ergs^{-1}cm^{-2})	Absorbed flux 6–8 keV	0.57 ± 0.01	⋯
	Flux fraction$_{6-8{\rm keV}}$ (%)	Disk contribution	33	⋯
kerrbb	η	Inner-torque modification	⋯	0 (frozen)
	a/M	BH spin	⋯	$0.49^{+0.07}_{-0.22}$
	i (deg)	Inclination	⋯	<21.2
	$M_{\rm BH}$ ($M_\odot$)	BH mass	⋯	10 (frozen)
	$\dot{M}$ (10^{18} g s^{-1})	Mass accretion rate	⋯	$4.0^{+0.8}_{-0.1}$
	D (kpc)	Distance	⋯	8 (frozen)
	hd	Hardening factor	⋯	1.7 (frozen)
powerlaw	Γ	Photon index	$2.9^{+0.8}_{-0.7}$	$3.1^{+0.3}_{-0.4}$
	norm	Normalization	$2.2^{+9.2}_{-1.6}$	$3.4^{+7.6}_{-2.6}$
	$F_{2-8{\rm keV}}$ (10^{-10}ergs^{-1}cm^{-2})	Absorbed flux 2–8 keV	4.01 ± 0.12	⋯
	Flux fraction$_{2-8{\rm keV}}$ (%)	Comptonized contribution	24	⋯
	$F_{2-6{\rm keV}}$ (10^{-10}ergs^{-1}cm^{-2})	Absorbed flux 2–6 keV	2.81 ± 0.09	⋯
	Flux fraction$_{2-6{\rm keV}}$ (%)	Comptonized contribution	19	⋯
	$F_{6-8{\rm keV}}$ (10^{-10}ergs^{-1}cm^{-2})	Absorbed flux 6–8 keV	1.20 ± 0.04	⋯
	Flux fraction$_{6-8{\rm keV}}$ (%)	Comptonized contribution	67	⋯
constant	$C_{\rm DU1}$	Normalization	0.89 ± 0.01	0.88 ± 0.01
	$C_{\rm DU2}$	Normalization	0.90 ± 0.01	0.90 ± 0.01
	$C_{\rm DU3}$	Normalization	0.87 ± 0.01	0.87 ± 0.01
	χ^2/dof		871/808	869/807

Note. Fluxes, corrected for absorption, have been computed convolving each component with the cflux model in XSPEC.

4.2. Spectral Fit

Due to the overall stability of the hardness ratio throughout the observation, we used time-averaged IXPE data for the subsequent spectral analysis in XSPEC. To further support this choice we initially performed separate fits of the spectra extracted before and after the count-rate drop on 2025 April 7, finding that the best-fit parameters are consistent within the 90% confidence level across all intervals. We performed a joint fit of the three IXPE Stokes I spectra in the 2–8 keV band together with the Swift/XRT spectrum in the 1–10 keV range. The fit statistics are presented in Table 2, while the unfolded spectra along with the data-model residuals are shown in Figure 3.

The spectrum of MAXI J1744−294 is well described by an absorbed disk blackbody with a minor contribution from a Comptonized component, consistent with the source being in the soft state. We fit the data employing a model consisting of a diskbb component (K. Mitsuda et al. 1984), representing a multitemperature blackbody accretion disk, and a powerlaw component to describe the high-energy tail. Interstellar absorption was modeled using the tbabs model with the relative abundances from J. Wilms et al. (2000). We additionally included a constant component in each fit to account for cross-calibration between Swift/XRT and the IXPE DUs. This constant was fixed at 1 for Swift, and left free to vary independently for the three IXPE DUs. The fit results in a χ^2/d.o.f. of 871/808. The inner disk temperature was 0.64 ± 0.01 keV, in agreement with the previous estimates by S. Mandel et al. (2025d, 2025e). For the interstellar absorption, we estimated a hydrogen column density of $N_{\rm H} = (19.2^{+0.6}_{-0.3}) \times 10^{22}$ cm^{-2}. This value is notably larger than initial estimates for the source ($N_{\rm H} \sim 11$–13×10^{22} cm^{-2}; S. Mandel et al. 2025d, 2025e; Y. Wang et al. 2025), likely due to the limited low-energy coverage of the instruments available in some of the early analyses, which reduces the sensitivity to the absorption column density. This value is consistent with more recent results from XRISM and XMM-Newton observations (Parra et al. 2026, in preparation; S. Mandel et al. 2025c). Due to the limited high-energy coverage of both instruments employed in our analysis, we find that both the photon index and the normalization of the powerlaw are largely unconstrained.

From this analysis, we estimate a 2–8 keV absorbed and unabsorbed flux of $(1.64 \pm 0.02) \times 10^{-9}$ erg s^{-1} cm^{-2} and $(1.04 \pm 0.01) \times 10^{-8}$ erg s^{-1} cm^{-2}, respectively.[28] Assuming a source distance of 8 kpc, consistent with its location near the Galactic center, this corresponds to an X-ray luminosity of $L_{\rm X} \sim 4 \times 10^{38}$ erg s^{-1}. In this empirical decomposition, the disk component dominates the spectrum below 6 keV, contributing approximately 81% of the total flux. At higher

[28] Fluxes have been estimated with the cflux model in XSPEC.

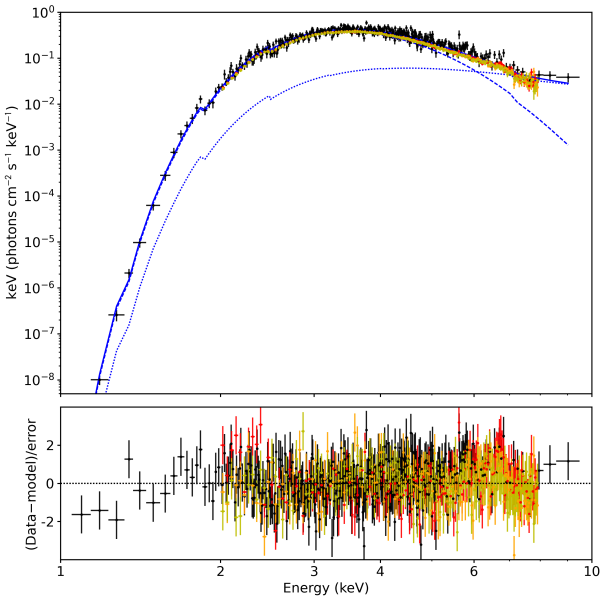

Figure 3. X-ray spectra of MAXI J1744−294, as observed by IXPE and Swift/XRT. Top panel: unfolded spectra (i.e., the flux $F(E)$) for the best-fit model. Swift/XRT data are shown in black, and the three IXPE DUs are shown in red, orange, and yellow, respectively. The blue curves represent the best-fit spectral model: The solid line indicates the total emission, while the dashed and dotted lines correspond to the disk and Comptonized components, respectively. Bottom panel: data minus model residuals in units of σ.
(The data used to create this figure are available in the online article.)

energies, the power-law component becomes more prominent, with the disk contributing only about 33% of the total flux between 6 and 8 keV. The flux values estimated for both the thermal and the Comptonized component in each energy range are reported in Table 2.

We also performed a spectral fit using the relativistic disk model `kerrbb` (L.-X. Li et al. 2005) in place of the simpler `diskbb`, to obtain a more physically motivated description of the accretion-disk emission. Because continuum-fitting methods suffer from strong degeneracies between spin, inclination, mass, and distance (R. A. Remillard & J. E. McClintock 2006), we fixed the source distance to $D = 8$ kpc and BH mass to $M = 10M_{\odot}$. We also adopted a standard disk hardening factor of 1.7 (T. Shimura & F. Takahara 1995). This model provides a good fit to the data, with $\chi^2/\mathrm{d.o.f.} = 869/807$. The fit yields a BH spin parameter of $a \approx 0.5$, while only resulting in an upper limit estimate for the inclination of $i \lesssim 21°$. However, we emphasize that the spin and the inclination are strongly degenerate and the associated systematic uncertainties far exceed the statistical errors listed in Table 2. These estimates are also sensitive to the assumed mass and distance. Tighter constraints on the physical parameters will require independent measurements of the source mass, distance, or inclination, or a more comprehensive analysis of the source broadband X-ray emission during the outburst (S. Mandel et al. 2025c).

4.3. Polarimetric Fit

We then incorporated the polarimetric information provided by IXPE into our fitting procedure. Keeping all spectral parameters fixed at the values listed in Table 2, we added the IXPE Q and U spectra to our analysis, applying the same cross-calibration factors used for the I spectrum. We assigned a constant PD and PA to the entire model using a `polconst` component, with only the PD and PA left as free parameters during the fit. We performed this analysis over the full IXPE energy range (2–8 keV), as well as in two smaller intervals: 2–6 keV and 6–8 keV. This choice is justified by the different flux contribution of the two spectral components in these two energy ranges, with the disk emission dominating at low energies, which is expected to be less polarized than the Comptonized radiation from the corona.

Figure 4 shows the resulting PD–PA contours, computed using the `steppar` command in XSPEC with 50 steps per parameter. Across all energy ranges, we find no significant polarization detection, consistent with the `PCUBE` results presented in Section 3. We derive upper limits on the PD of $<1.3\%$ (at 3σ confidence) for both the 2–8 keV and 2–6 keV bands. Notably, the upper limit obtained for the full IXPE band is significantly lower than that from the `PCUBE` analysis presented in Section 3. This difference is due to the weighted fitting approach applied in this spectro-polarimetric analysis (A. Di Marco et al. 2022).

In the 6–8 keV band, however, we find an interesting hint of a polarization signal. The best-fit values are PD $= 7.8\% \pm 3.6\%$ and PA $= 2° \pm 16°$, where the 1σ uncertainties are calculated here as the extreme values of the contour plot shown in the right panel of Figure 4. As the contour at 3σ, plotted as solid lines in Figure 4, is not closed, we do not consider this a solid detection but rather interesting information to report for further studies.

5. Discussion

In this study, we have presented the first X-ray spectro-polarimetric analysis of MAXI J1744−294. This transient source, observed during a bright 2025 outburst near the Galactic center, has been the focus of an intensive observational campaign across multiple wavelengths (N. Grollimund et al. 2025; C. O. Heinke et al. 2025; G. K. Jaisawal et al. 2025; Y. Kudo et al. 2025; S. Mandel et al. 2025b, 2025d, 2025e; M. Nakajima et al. 2025; Y. Wang et al. 2025; S. Watanabe et al. 2025). Our IXPE observation, conducted approximately 3 months after the outburst discovery, adds a new piece to this effort through X-ray polarimetry. At the time of the observation, the source was in the soft state, with the emission well modeled by a heavily absorbed multicolor disk component and a weak power-law component extending to the hard X-rays. The X-ray flux showed a slow decline over the ∼150 ks exposure, hinting at the source entering the decay phase of the outburst.

The X-ray emission from MAXI J1744−294 was found to be unpolarized, with a 1.3% 3σ upper limit on the PD in both the full 2–8 keV band and the 2–5 keV range, where the disk component dominates the flux.

This polarization measurement is consistent with previous IXPE observations of accreting BH XRBs in the soft state. In general, sources observed in this spectral state have shown very low PD, with several measurements resulting in upper limits: for instance, LMC X-1 (PD <2.5%; J. Podgorný et al. 2023), Swift J1727.8−1613 (PD <1.1%; J. Svoboda et al. 2024a), and GX 339−4 (PD <1.4%; G. Mastroserio et al. 2025). The case of Swift J1727.8−1613 is particularly illustrative, as the source was tracked throughout its outburst by IXPE, allowing for the first time the observation of a progressive decrease in PD as the spectrum softened (A. Ingram et al. 2024; J. Svoboda et al. 2024a). Polarization

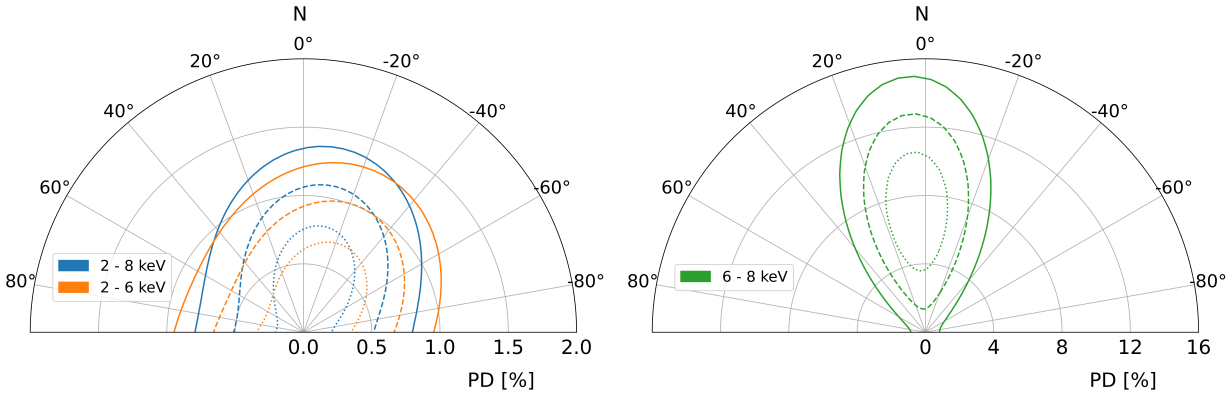

Figure 4. Polar plot of the PD and PA, assuming the best-fit spectral model. Left: results for the full IXPE energy band (2–8 keV) and the 2–6 keV interval. Right: results for the 6–8 keV interval. Dotted, dashed, and solid lines represent the 1σ, 2σ, and 3σ confidence contours, respectively.

detections in the soft state have so far been limited to a few sources, typically characterized by large (measured or inferred) inclination angles between the observer's line of sight and the disk axis. Notable examples include LMC X-3 ($i \approx 69°$; J. Svoboda et al. 2024b), 4U 1957+11 ($i \sim 50°$–$75°$; L. Marra et al. 2024), and 4U 1630−47 ($i \sim 65°$; A. Ratheesh et al. 2024). An exception to this trend is Cyg X-1, for which a significant polarization signal was detected in the soft state (J. F. Steiner et al. 2024) despite its relatively low binary inclination ($i \approx 27°$; J. A. Orosz et al. 2011). However, it has been proposed that the innermost accretion disk in this system may be misaligned with the binary plane, leading to a higher effective inclination that could explain the observed polarization, particularly during the hard state (H. Krawczynski et al. 2022, but see also J. Poutanen et al. 2023; V. Kravtsov et al. 2025).

Disk inclination is a leading factor influencing the PD of the thermal X-ray emission from accretion disks around stellar-mass BHs (M. Dovčiak et al. 2008; J. D. Schnittman & J. H. Krolik 2009). This dependence arises from the axisymmetric geometry of the disk: For a face-on configuration ($i = 0°$), the symmetry leads to complete cancellation of the polarization vectors, resulting in a zero net polarization. As the viewing angle increases toward an edge-on orientation ($i = 90°$), this symmetry is progressively lost, leading to stronger net polarization signals. In the case of MAXI J1744−294, robust constraints on the disk inclination remain limited. However, our measured upper limit on the PD provides a useful observational constraint. By comparing this limit with theoretical predictions, we can place an initial constraint on the range of viewing angles for the system. We stress that this analysis provides only a first, qualitative estimate of the source inclination, since it relies on the estimate of a PD upper limit and involves several assumptions on the accretion-disk structure and on the physical parameters of the source (see Section 4.2).

In the soft-state sources, the observed X-ray polarization presumably arises from Thomson scattering in the optically thick accretion-disk atmosphere (M. Dovčiak et al. 2008; R. Taverna et al. 2021). This process can be modeled using classical results derived for pure electron-scattering, semi-infinite atmospheres (S. Chandrasekhar 1960; V. V. Sobolev 1963). Additionally, in the BH vicinity, relativistic effects are expected to significantly alter the spectro-polarimetric properties of the emerging radiation (P. A. Connors & R. F. Stark 1977; R. F. Stark & P. A. Connors 1977; P. A. Connors et al. 1980; M. Dovčiak et al. 2008; R. Taverna et al. 2020; V. Loktev et al. 2024). These effects lead to a net depolarization of the signal and introduce the additional contribution from the returning radiation (i.e., photons emitted by the disk that are gravitationally bent and re-interact with the disk surface before reaching the observer; J. D. Schnittman & J. H. Krolik 2009). Returning photons are expected to scatter off the disk surface and become polarized along the disk axis, while photons emerging from the optically thick atmosphere and directly reaching the observer are predicted to be polarized perpendicularly to the disk axis (M. Dovčiak et al. 2008; R. Taverna et al. 2021).

To model these effects, we adopt the KYNBBRR model (M. Dovčiak et al. 2008; R. Taverna et al. 2020; R. Mikusincova et al. 2023), a relativistic ray-tracing code that simulates the spectro-polarimetric emission from BH accretion disks. The model assumes a standard Novikov–Thorne (I. D. Novikov & K. S. Thorne 1973) disk with self-irradiation and allows us to study the variation of the observed Stokes parameters, depending on the BH spin, the system inclination, and the disk atmosphere albedo, which determines the amount of returning radiation contributing to the observed spectra. This model has been successfully used to model the spectro-polarimetric properties of the accretion-disk emission in sources observed in soft state like LMC X-3 (J. Svoboda et al. 2024b) and 4U 1957+11 (L. Marra et al. 2024). Moreover, it was applied to analyze the soft-state IXPE observation of 4U 1630−47 (A. Ratheesh et al. 2024), although it could not reproduce the very large PD observed in this source.

Figure 5 shows the dependence of the observed PD on the inclination angle, as predicted by the KYNBBRR model for various BH spin values. The model was convolved with a TBABS component in XSPEC in order to take into consideration the large interstellar absorption characterizing this source. We fixed the hydrogen column density, the BH mass, its distance, and its accretion rate to the values obtained in the KERRBB spectral fit, as detailed in Table 2. The Stokes parameters were integrated over the 2–6 keV band, where the disk emission is the main contributor to the flux. Two limiting cases for the disk surface albedo were considered: albedo = 0, corresponding to full absorption of returning radiation, and albedo = 1, where all returning radiation is reflected with no absorption. The model predictions are compared to the measured 3σ upper limit on the PD in this energy band, with

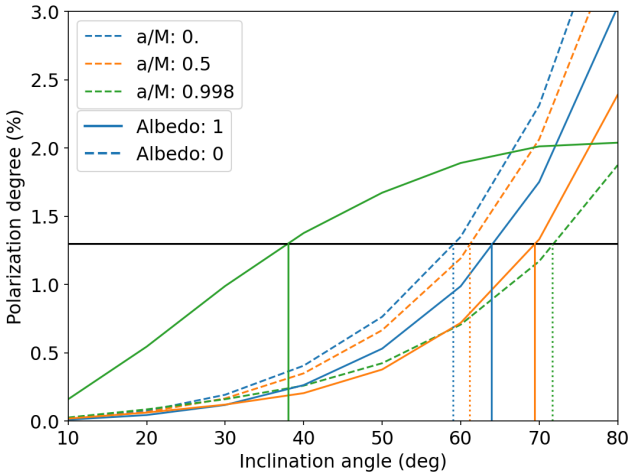

Figure 5. Modeling of the PD predicted by the relativistic accretion-disk model KYNBBRR in the 2–6 keV energy range for different BH spin values: $a/M = 0$ (blue), 0.5 (orange), and 0.998 (green). Solid lines correspond to albedo = 1, and dashed lines correspond to albedo = 0. The horizontal black line indicates the observed PD upper limit at the 3σ confidence level. Vertical dotted lines mark the maximum inclination allowed by the simulations for albedo 0 (59°, 61°, and 72° for $a/M = 0$, 0.5, and 0.998, respectively) while vertical solid lines show the corresponding limits for albedo 1 (63.°8, 69.°4, and 38° for $a/M = 0$, 0.5, and 0.998, respectively), based on intersections with the 3σ line.

the intersections representing upper limits on the inclination angle. When no returning radiation is included (albedo = 0), the energy-integrated PD decreases with increasing BH spin due to stronger relativistic depolarization effects. The corresponding inclination upper limits are $i < 59°$, 61°, and 72° for spin parameters $a/M = 0$, 0.5, and 0.998, respectively.

The inclusion of returning radiation contribution (albedo = 1) results in the predicted PD decreasing when the BH spin is 0 or 0.5, due to the mixing of two orthogonally polarized contributions. Conversely, for a rapidly spinning BH ($a/M = 0.998$), due to the disk extending much closer to the BH, a larger fraction of photons emitted by the disk are gravitationally bent back onto the disk surface before reaching the observer. This makes the returning radiation contribution increasingly dominant already in the 2–6 keV band, leading to an overall increase in the predicted PD. In this configuration, the inferred inclination limits are $i < 63.°8$, $69.°4$, and 38° for spin values of 0, 0.5, and 0.998, respectively. Although these constraints should be interpreted with caution, given the underlying model assumptions and the absence of a significant polarization detection, this analysis of the polarimetric data suggests that MAXI J1744−294 is observed at a relatively low/intermediate inclination angle, in agreement with the fact that no eclipses, dips in the X-ray light curves, or wind signatures in the X-ray spectra have been observed to date. If MAXI J1744−294 is associated with the 2016 transient Swift J174540.2−290037, reflection-based spectral modeling of that outburst suggested a relatively low disk inclination of ∼20°–30° (K. Mori et al. 2019), consistent with the inclination range inferred from our polarimetric constraints.

6. Conclusions

We presented the first IXPE spectro-polarimetric observation of the BH candidate MAXI J1744−294 during its 2025 outburst. Recent work suggests that this event may correspond to a repeat outburst of the 2016 transient Swift J174540.2−290037. The source was observed in the soft state, with a spectrum dominated by a multicolor disk and a weak Comptonized tail. No significant polarization signal was detected, and we derived a 3σ upper limit of 1.3% on the PD in both the 2–8 keV and 2–6 keV bands. This result is consistent with previous IXPE measurements of low to moderate inclination BH XRBs in similar states. By comparing our PD upper limit with the theoretical prediction from relativistic disk models, we tentatively constrain the inclination of the system to $i \lesssim 38°$–72°, depending on the BH spin and disk atmosphere albedo. Our findings, in line with other IXPE observations, confirm the trend of low polarization signals in sources observed in soft state and underscore the role of X-ray polarimetry in revealing key aspects of BH accretion geometry.

Acknowledgments

The Imaging X-ray Polarimetry Explorer (IXPE) is a joint US and Italian mission. The US contribution is supported by the National Aeronautics and Space Administration (NASA) and led and managed by its Marshall Space Flight Center (MSFC), with industry partner Ball Aerospace (contract NNM15AA18C). The Italian contribution is supported by the Italian Space Agency (Agenzia Spaziale Italiana, ASI) through contract ASI-OHBI-2022-13-I.0, agreements ASI-INAF-2022-19-HH.0 and ASI-INFN-2017.13-H0, and its Space Science Data Center (SSDC) with agreements ASI-INAF-2022-14-HH.0 and ASI-INFN 2021-43-HH.0, and by the Istituto Nazionale di Astrofisica (INAF) and the Istituto Nazionale di Fisica Nucleare (INFN) in Italy. This research used data products provided by the IXPE Team (MSFC, SSDC, INAF, and INFN) and distributed with additional software tools by the High-Energy Astrophysics Science Archive Research Center (HEASARC), at NASA Goddard Space Flight Center (GSFC).

L.M., F.M., P.S., G.Matt, and R.T. acknowledge support from the project PRIN 2022–2022LWPEXW, "An X-Ray View of Compact Objects in Polarized Light," European Union funding, Next Generation EU, Mission 4, Component 1, CUP C53D23001180006. F.M.V. is supported by the European Union's Horizon Europe research and innovation program through the Marie Skłodowska-Curie grant agreement No. 101149685. F.C. and A.T. acknowledge financial support from the Istituto Nazionale di Astrofisica (INAF) grant No. 1.05.23.05.06, "Spin and Geometry in Accreting X-Ray Binaries: The First Multi-frequency Spectro-polarimetric Campaign." M.D.S. and A.D. acknowledge ASI-INAF program I/004/11/6 (Swift) and funding from the European Union, Next Generation EU, Mission 4, Component 1, CUP C53D23001330006 (PRIN MUR 2022 SEAWIND project No. 2022Y2T94C). S.F. acknowledges financial support from the Istituto Nazionale di Astrofisica (INAF) grant No. 1.05.24.02.04: "A Multi-frequency Spectro-polarimetric Campaign to Explore Spin and Geometry in Low Mass X-Ray Binaries." M.D., M.G., J.Pod., and J.S. thank GACR project 21-06825X for the support and institutional support from RVO:67985815. V.E.G. acknowledges funding under NASA contract 80NSSC24K1403. A.I. acknowledges support from the Royal Society. P.O.P. acknowledges financial support from the CNRS, "Action Thématique Processus Extrêmes et Multimessagers," and from the CNES, the French Space

Agency. A.V. acknowledges support from the Academy of Finland grant No. 355672. Nordita is supported in part by NordForsk. A.G. was supported by an appointment to the NASA Postdoctoral Program at the Marshall Space Flight Center (MSFC), administered by Oak Ridge Associated Universities under contract with NASA.

Facilities: IXPE, Swift (XRT), NICER.

Software: DS 9 (Smithsonian Astrophysical Observatory 2000), HEASoft v6.35 (NASA High Energy Astrophysics Science Archive Research Center [HEASARC] 2014), IXPEOBSSIM (L. Baldini et al. 2022), XSPEC v12.15 (K. A. Arnaud 1996).

ORCID iDs

Lorenzo Marra https://orcid.org/0009-0001-4644-194X
Romana Mikušincová https://orcid.org/0000-0001-7374-843X
Federico M. Vincentelli https://orcid.org/0000-0002-1481-1870
Fiamma Capitanio https://orcid.org/0000-0002-6384-3027
Melania Del Santo https://orcid.org/0000-0002-1793-1050
Sergio Fabiani https://orcid.org/0000-0003-1533-0283
Shifra Mandel https://orcid.org/0000-0002-6126-7409
Fabio Muleri https://orcid.org/0000-0003-3331-3794
Maxime Parra https://orcid.org/0009-0003-8610-853X
Paolo Soffitta https://orcid.org/0000-0002-7781-4104
Antonella Tarana https://orcid.org/0009-0007-0537-9805
M. Cristina Baglio https://orcid.org/0000-0003-1285-4057
Stefano Bianchi https://orcid.org/0000-0002-4622-4240
Stéphane Corbel https://orcid.org/0000-0001-5538-5831
Enrico Costa https://orcid.org/0000-0003-4925-8523
Antonino D'Aì https://orcid.org/0000-0002-5042-1036
Barbara De Marco https://orcid.org/0000-0003-2743-6632
Michal Dovčiak https://orcid.org/0000-0003-0079-1239
Vittoria Elvezia Gianolli https://orcid.org/0000-0002-9719-8740
Andrea Gnarini https://orcid.org/0000-0002-0642-1135
Maitrayee Gupta https://orcid.org/0000-0003-0976-8932
Adam Ingram https://orcid.org/0000-0002-5311-9078
Guglielmo Mastroserio https://orcid.org/0000-0003-4216-7936
Giorgio Matt https://orcid.org/0000-0002-2152-0916
Kaya Mori https://orcid.org/0000-0002-9709-5389
Pierre-Olivier Petrucci https://orcid.org/0000-0001-6061-3480
Jakub Podgorný https://orcid.org/0000-0001-5418-291X
Juri Poutanen https://orcid.org/0000-0002-0983-0049
James F. Steiner https://orcid.org/0000-0002-5872-6061
Jiří Svoboda https://orcid.org/0000-0003-2931-0742
Roberto Taverna https://orcid.org/0000-0002-1768-618X
Francesco Tombesi https://orcid.org/0000-0002-6562-8654
Swati Ravi https://orcid.org/0000-0002-2381-4184
Jérôme Rodriguez https://orcid.org/0000-0002-4151-4468
Thomas D. Russell https://orcid.org/0000-0002-7930-2276
Alexandra Veledina https://orcid.org/0000-0002-5767-7253
Shuo Zhang https://orcid.org/0000-0002-2967-790X

References

Alabarta, K., Altamirano, D., Méndez, M., et al. 2021, MNRAS, 507, 5507
Arnaud, K. A. 1996, ASPC, 101, 17
Baldini, L., Barbanera, M., Bellazzini, R., et al. 2021, APh, 133, 102628
Baldini, L., Bucciantini, N., Lalla, N. D., et al. 2022, SoftX, 19, 101194
Bassi, T., Del Santo, M., D'Aı, A., et al. 2019, MNRAS, 482, 1587
Belczynski, K., Bulik, T., Fryer, C. L., et al. 2010, ApJ, 714, 1217
Belloni, T., Homan, J., Casella, P., et al. 2005, A&A, 440, 207
Belloni, T. M. 2010, LNP, 794, 53
Burrows, D. N., Hill, J. E., Nousek, J. A., et al. 2005, SSRv, 120, 165
Capitanio, F., Belloni, T., Del Santo, M., & Ubertini, P. 2009, MNRAS, 398, 1194
Chandrasekhar, S. 1960, Radiative Transfer (Dover)
Connors, P. A., Piran, T., & Stark, R. F. 1980, ApJ, 235, 224
Connors, P. A., & Stark, R. F. 1977, Natur, 269, 128
Corral-Santana, J. M., Casares, J., Muñoz-Darias, T., et al. 2016, A&A, 587, A61
Degenaar, N., Wijnands, R., Miller, J. M., et al. 2015, JHEAp, 7, 137
Del Santo, M., Belloni, T. M., Homan, J., et al. 2009, MNRAS, 392, 992
Di Marco, A., Costa, E., Muleri, F., et al. 2022, AJ, 163, 170
Di Marco, A., Soffitta, P., Costa, E., et al. 2023, AJ, 165, 143
Done, C., Gierliński, M., & Kubota, A. 2007, A&ARv, 15, 1
Dovčiak, M., Muleri, F., Goosmann, R. W., Karas, V., & Matt, G. 2008, MNRAS, 391, 32
Dovčiak, M., Podgorný, J., Svoboda, J., et al. 2024, Galax, 12, 54
Dunn, R. J. H., Fender, R. P., Körding, E. G., Belloni, T., & Cabanac, C. 2010, MNRAS, 403, 61
Ewing, M., Parra, M., Mastroserio, G., et al. 2025, MNRAS, 541, 1774
Fender, R. P., Belloni, T. M., & Gallo, E. 2004, MNRAS, 355, 1105
Ferrazzoli, R., Costa, E., Fabiani, S., et al. 2025, AJ, 170, 325
Fortin, F., Kalsi, A., García, F., Simaz-Bunzel, A., & Chaty, S. 2024, A&A, 684, A124
Grollimund, N., Corbel, S., Bahramian, A., et al. 2025, ATel, 17045, 1
Hailey, C. J., Mori, K., Bauer, F. E., et al. 2018, Natur, 556, 70
Heinke, C. O., Nakajima, M., Kudo, Y., et al. 2025, ATel, 17010, 1
Homan, J., & Belloni, T. 2005, Ap&SS, 300, 107
Ingram, A., Bollemeijer, N., Veledina, A., et al. 2024, ApJ, 968, 76
Jaisawal, G. K., Steiner, J. F., Strohmayer, T. E., et al. 2025, ATel, 17040, 1
King, A. R., Kolb, U., & Burderi, L. 1996, ApJL, 464, L127
Kislat, F., Clark, B., Beilicke, M., & Krawczynski, H. 2015, APh, 68, 45
Kravtsov, V., Bocharova, A., Veledina, A., et al. 2025, A&A, 701, A115
Krawczynski, H., & Beheshtipour, B. 2022, ApJ, 934, 4
Krawczynski, H., Muleri, F., Dovčiak, M., et al. 2022, Sci, 378, 650
Kudo, Y., Negoro, H., Nakajima, M., et al. 2025, ATel, 16975, 1
Li, L.-X., Zimmerman, E. R., Narayan, R., & McClintock, J. E. 2005, ApJS, 157, 335
Loktev, V., Veledina, A., Poutanen, J., Nättilä, J., & Suleimanov, V. F. 2024, A&A, 685, A84
Maccarone, T. J., & Coppi, P. S. 2003, MNRAS, 338, 189
Makishima, K., Maejima, Y., Mitsuda, K., et al. 1986, ApJ, 308, 635
Mandel, S., Gerber, J., Mori, K., et al. 2025a, ApJ, 985, 202
Mandel, S., Levin, B., Mori, K., et al. 2025b, ATel, 17087, 1
Mandel, S., Mori, K., Ciurlo, A., et al. 2025c, arXiv:2509.14465
Mandel, S., Mori, K., Hailey, C., et al. 2025d, ATel, 17031, 1
Mandel, S., Mori, K., Hailey, C., et al. 2025e, ATel, 17063, 1
Mandel, S., Mori, K., Hua, Z., et al. 2026, ATel, 17663, 1
Mariani, I., Motta, S. E., Baglio, M. C., et al. 2025, ATel, 17164, 1
Marin, F., Churazov, E., Khabibullin, I., et al. 2023, Natur, 619, 41
Marra, L., Brigitte, M., Rodriguez Cavero, N., et al. 2024, A&A, 684, A95
Mastroserio, G., De Marco, B., Baglio, M. C., et al. 2025, ApJL, 978, L19
Matsuoka, M., Kawasaki, K., Ueno, S., et al. 2009, PASJ, 61, 999
Meyer-Hofmeister, E., Liu, B. F., & Meyer, F. 2005, A&A, 432, 181
Mikusincova, R., Dovciak, M., Bursa, M., et al. 2023, MNRAS, 519, 6138
Mikušincová, R., Marra, L., Manikantan, H., et al. 2025, arXiv:2512.13182
Mitsuda, K., Inoue, H., Koyama, K., et al. 1984, PASJ, 36, 741
Mori, K., Hailey, C. J., Mandel, S., et al. 2019, ApJ, 885, 142
Mori, K., Hailey, C. J., Schutt, T. Y. E., et al. 2021, ApJ, 921, 148
Muno, M. P., Pfahl, E., Baganoff, F. K., et al. 2005, ApJL, 622, L113
Nakajima, M., Negoro, H., Kudo, Y., et al. 2025, ATel, 16983, 1
NASA High Energy Astrophysics Science Archive Research Center (Heasarc) 2014, HEAsoft: Unified Release of FTOOLS and XANADU, ascl:1408.004
Novikov, I. D., & Thorne, K. S. 1973, Astrophysics of Black Holes, in Black Holes (Les Astres Occlus), ed. C. DeWitt & D. DeWitt (Gordon and Breach), 343
Orosz, J. A., McClintock, J. E., Aufdenberg, J. P., et al. 2011, ApJ, 742, 84
Page, D. N., & Thorne, K. S. 1974, ApJ, 191, 499
Parra, M., Petrucci, P. O., Bianchi, S., et al. 2024, A&A, 681, A49
Podgorný, J., Marra, L., Muleri, F., et al. 2023, MNRAS, 526, 5964

Podgorný, J., Svoboda, J., Dovčiak, M., et al. 2024, A&A, 686, L12
Ponti, G., Fender, R. P., Begelman, M. C., et al. 2012, MNRAS, 422, L11
Poutanen, J., & Svensson, R. 1996, ApJ, 470, 249
Poutanen, J., Veledina, A., & Beloborodov, A. M. 2023, ApJL, 949, L10
Ramsey, B. D., Bongiorno, S. D., Kolodziejczak, J. J., et al. 2022, JATIS, 8, 024003
Ratheesh, A., Dovčiak, M., Krawczynski, H., et al. 2024, ApJ, 964, 77
Remillard, R. A., & McClintock, J. E. 2006, ARA&A, 44, 49
Rodriguez Cavero, N., Marra, L., Krawczynski, H., et al. 2023, ApJL, 958, L8
Schnittman, J. D., & Krolik, J. H. 2009, ApJ, 701, 1175
Schnittman, J. D., & Krolik, J. H. 2010, ApJ, 712, 908
Shakura, N. I., & Sunyaev, R. A. 1973, A&A, 24, 337
Shimura, T., & Takahara, F. 1995, ApJ, 445, 780
Smithsonian Astrophysical Observatory 2000, SAOImage DS9: A utility for displaying astronomical images in the X11 window environment, Astrophysics Source Code Library, ascl:0003.002
Sobolev, V. V. 1963, A Treatise on Radiative Transfer (Van Nostrand-Reinhold)
Soffitta, P., Baldini, L., Bellazzini, R., et al. 2021, AJ, 162, 208
Stark, R. F., & Connors, P. A. 1977, Natur, 266, 429
Steiner, J. F., Nathan, E., Hu, K., et al. 2024, ApJL, 969, L30
Sunyaev, R. A., & Truemper, J. 1979, Natur, 279, 506
Svoboda, J., Dovčiak, M., Steiner, J. F., et al. 2024a, ApJL, 966, L35
Svoboda, J., Dovčiak, M., Steiner, J. F., et al. 2024b, ApJ, 960, 3
Taverna, R., Marra, L., Bianchi, S., et al. 2021, MNRAS, 501, 3393
Taverna, R., Zhang, W., Dovčiak, M., et al. 2020, MNRAS, 493, 4960
Tetarenko, B. E., Sivakoff, G. R., Heinke, C. O., & Gladstone, J. C. 2016, ApJS, 222, 15
Thorne, K. S., & Price, R. H. 1975, ApJL, 195, L101
Uttley, P., Cackett, E. M., Fabian, A. C., Kara, E., & Wilkins, D. R. 2014, A&ARv, 22, 72
Veledina, A., Muleri, F., Dovčiak, M., et al. 2023, ApJL, 958, L16
Veledina, A., Muleri, F., Poutanen, J., et al. 2024a, NatAs, 8, 1031
Veledina, A., Poutanen, J., Bocharova, A., et al. 2024b, A&A, 688, L27
Wang, Y., Coti Zelati, F., Rea, N., et al. 2025, ATel, 17068, 1
Watanabe, S., Aoyama, A., Takeda, T., et al. 2025, ATel, 17009, 1
Weisskopf, M. C., Elsner, R. F., & O'Dell, S. L. 2010, SPIE, 7732, 77320E
Weisskopf, M. C., Soffitta, P., Baldini, L., et al. 2022, JATIS, 8, 026002
Wilms, J., Allen, A., & McCray, R. 2000, ApJ, 542, 914
Yu, W., & Yan, Z. 2009, ApJ, 701, 1940
Zdziarski, A. A., & Gierliński, M. 2004, PThPS, 155, 99
Zhang, W., Dovčiak, M., Bursa, M., et al. 2022, MNRAS, 515, 2882